Mesoscopic Multiparticle Collision Dynamics of Reaction−Diffusion Fronts†

Kay Tucci

SUMA-CeSiMo, Universidad de Los Andes, Mérida 5101, Venezuela

Raymond Kapral*

Chemical Physics Theory Group, Department of Chemistry, University of Toronto, Toronto, ON M5S 3H6, Canada

Received: May 23, 2005

A mesoscopic multiparticle collision model for fluid dynamics is generalized to incorporate the chemical reactions among species that may diffuse at different rates. This generalization provides a means to simulate reaction−diffusion dynamics of complex reactive systems. The method is illustrated by a study of cubic autocatalytic fronts. The mesoscopic scheme is able to reproduce the results of reaction−diffusion descriptions under conditions where the mean field equations are valid. The model is also able to incorporate the effects of molecular fluctuations on the reactive dynamics.

1. Introduction

Mesoscopic models provide coarse-grained descriptions of the dynamics of systems that neglect certain details at microscopic scales while retaining essential dynamical features at mesoscopic and macroscopic scales. Consequently, a convenient way to study of the dynamics of complex systems over a large range of interesting space and time scales is through the use of such models. In physical and biological systems we often encounter situations where mean field descriptions of reactions break down and molecular fluctuations play an important role in determining the character of the system's dynamics. Such effects are especially relevant for reactions taking place in nanoscale domains or biochemical reactions at the cellular level. Fluctuations also play a role in far-from-equilibrium systems near bifurcation points or when the system behaves chaotically since the system is especially susceptible to perturbations in such regimes.[1] Mesoscopic models are able to capture the influence of such molecular fluctuations on the dynamics. Mesoscopic models are also useful for simulating the dynamics of macroscopic systems because they often provide stable particle-based simulation schemes and can be implemented in complex geometries.

In this article we consider a generalization of a mesoscopic multiparticle collision (MPC) (or stochastic rotation) model[2−4] to a pattern-forming chemically reacting system. We show how the multiparticle collision rule can be generalized to a multicomponent system to yield different diffusion coefficients for the chemical species. Differences in diffusion coefficients can give rise to chemical instabilities which cannot occur if the diffusion coefficients of all species are equal. Reactions are incorporated, also at a mesoscopic level, by combining a birth−death description of reactive events with multiparticle collisions. The mesoscopic dynamics preserves all the basic conservation laws of the system and leads to the macroscopic evolution laws on long distance and time scales.

To illustrate the scheme, the reactive MPC dynamics is used to investigate the evolution and structure of a cubic autocatalytic front. The cubic autoatalytic reaction is A + 2B → 3B, where the autocatalyst B consumes the fuel A. If one considers a two-dimensional rectangular domain (or a thin rectangular slab in three dimensions) with B in left portion and A in the right portion, a reaction front will propagate from left to right. While the simulations presented in this paper are for cubic autocatalytic fronts, the manner in which the diffusion process is modeled to yield different diffusion coefficients for different chemical species and the way reactions are incorporated in the model presage extensions of the theory and applications to more complex far-from-equilibrium reactive systems.

The paper is organized as follows: In section 2 we sketch the basic elements of the multiparticle collision model and present its generalization to reactive systems where the chemical species can have different diffusion coefficients. Section 3 describes the simulation of cubic autocatalytic fronts and compares the results of the mesoscopic simulations with the predictions of reaction−diffusion equations. The conclusions of the paper are given in section 4.

2. Mesoscopic Model

In multiparticle collision dynamics, a system containing N particles with continuous positions $\boldsymbol{r}_i$ and velocities $\boldsymbol{v}_i$ evolves through a sequence of free streaming and collision steps.[3] The collisions among the particles take place in the following way: the system is divided into cells and at time intervals τ each cell labeled by ξ is assigned at random a rotation operator $\hat{\omega}_\xi$ from some suitable set of rotation operators. The center of mass velocity $\mathbf{V}_\xi$ of the particles in cell ξ is computed, and the post-collision velocity $\boldsymbol{v}'_i$ of particle i in the cell is determined by rotating its velocity, relative to the cell center of mass velocity, and adding the center of mass velocity to the result of this rotation

$$\boldsymbol{v}'_i = \boldsymbol{V}_\xi + \hat{\omega}_\xi(\boldsymbol{v}_i - \boldsymbol{V}_\xi) \tag{1}$$

The velocity of every particle in cell ξ is rotated by the same rotation operator, but the rotation operator varies from cell to cell. The dynamics then consists of free streaming interspersed

† Part of the special issue "Irwin Oppenheim Festschrift".

10.1021/jp052701u CCC: $30.25
Published on Web 07/01/2005

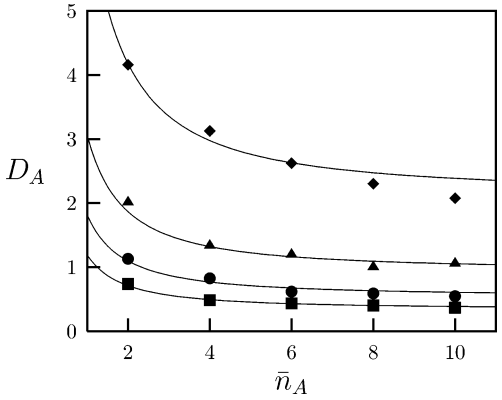

Figure 1. Diffusion coefficient $D_A(\gamma_A)$ as a function of the density $\bar{n}_A$ for various values of γ_A. Squares, $\gamma_A = 1.00$. Circles, $\gamma_A = 0.75$. Triangles, $\gamma_A = 0.50$. Diamonds $\gamma_A = 0.25$. Solid lines plot the theoretical value (eq 5) of the diffusion coefficient.

by these multiparticle collision events. It has been shown that this dynamics conserves mass, momentum, and energy and thus leads to the full set of Navier−Stokes equations on long distance and time scales.[3−5] The method has been applied to the study of a variety of systems[5] including hydrodynamic flows,[6] colloids,[7] polymers,[8] Brownian motion,[9] and simple diffusion-influenced reaction dynamics.[10]

We present a generalization of this model that allows the dynamics of reaction−diffusion systems to be investigated. This generalization entails several extensions of the MPC model. In particular, a multicomponent version of the MPC model[10,11] must be constructed that accounts for reactions among the chemical species and allows for the possibility that the diffusion coefficients of the species differ.

Diffusion. A multicomponent MPC dynamics that provides a simple way to control the diffusion coefficients of different chemical species can be constructed as follows. Suppose we have s species labeled by an index α. Instead of applying the MPC operator to all particles in a cell, we assume that multiparticle collision operators act to change the velocities of a fraction of the particles of species α in a cell for $\alpha = 1, ..., s$. More specifically, in each cell ξ, each particle of species α is chosen with probability γ_α. If $\boldsymbol{v}_i^\alpha$ is the velocity of a chosen particle i of species α and $\boldsymbol{V}_\xi^c$ is the center of mass velocity of all chosen particles, the post-collision velocities of those particles that undergo collision are given by

$$\mathbf{v}^{\alpha'}{}_i = \mathbf{V}_\xi{}^c + \hat{\omega}_\xi(\mathbf{v}_i{}^\alpha - \mathbf{V}_\xi{}^c) \tag{2}$$

The post-collision velocities of the particles that do not take part in the multiparticle collision do not change. The diffusion coefficients D_α are functions of $\{\gamma_{\alpha'}|\alpha' = 1, ..., s\}$, which can be tuned to change the values of the diffusion coefficients.

To investigate the range over which the diffusion coefficients can vary, we consider the self-diffusion coefficient of a single species A and change both the mean particle density $\bar{n}_A$ and the fraction γ_A of particles that participate in the multiparticle collisions. Figure 1 plots $D_A(\gamma_A)$, determined from the slope of the mean square displacement versus time, as a function density $\bar{n}_A$ for different values of γ_A. From these results one sees that the self-diffusion coefficient can be varied by about a factor of 5 by changing the values of γ_A at a fixed density.

The self-diffusion coefficient for $\gamma_A \neq 1$ can be estimated in the Boltzmann approximation where correlations are neglected. The discrete-time Green−Kubo expression for the diffusion coefficient is[4,10]

$$D_A(\gamma_A) = \frac{1}{2}\langle v_x{}^2\rangle + \sum_{n=1}^{\infty}\langle v_x(n)v_x\rangle \tag{3}$$

where, without loss of generality, we have set $\tau = 1$. Taking into account the collision rule where, on average, a fraction γ_A of the particles undergo multiparticle collisions and fraction $1 - \gamma_A$ do not, we have

$$D_A(\gamma_A) = \frac{1}{2}\langle v_x{}^2\rangle + (1 - \gamma_A)\langle v_x{}^2\rangle + \gamma_A\langle v_x{}^{(1)}v_x\rangle + ... \tag{4}$$

where $v^{(1)}{}_x$ is the post-collision value of the velocity at time $\tau = 1$. Assuming that higher order collision terms can be expressed in terms of the first collision so the series is geometric, we obtain

$$\begin{aligned} D_A(\gamma_A) &= -\frac{1}{2}\langle v_x{}^2\rangle + \langle v_x{}^2\rangle(1 + (1 - \gamma_A) + \gamma_A r_D + ...) \\ &\approx -\frac{1}{2}\langle v_x{}^2\rangle + \frac{\langle v_x{}^2\rangle}{\gamma_A(1 - r_D)} \\ &= \frac{\langle v_x{}^2\rangle}{2}\left[\frac{2 - \gamma_A(1 - r_D)}{\gamma_A(1 - r_D)}\right] \end{aligned} \tag{5}$$

where

$$r_D = \frac{\langle v_x{}^{(1)}v_x\rangle}{\langle v_x{}^2\rangle} = \frac{2(1 - e^{-\bar{n}_A}) + \bar{n}_A}{3\bar{n}_A} \tag{6}$$

was computed in ref 10. The comparison in Figure 1 shows that this analytical expression (solid lines) accurately describes the simulation data.

Reaction. The mesoscopic dynamics must also be generalized to allow for chemical reactions among the species. Our earlier study of diffusion-influenced reactions[10] was restricted to a simple $A + C \rightleftharpoons B + C$ reaction that occurs when the A or B particles collide with catalytic spheres C. Since we are now interested in reactions that occur among the mesoscopic particles, we instead use a birth−death stochastic law to describe the reactive events.[1,12]

Here we restrict our considerations to the cubic autocatalytic reaction $A + 2B \rightarrow 3B$. Independently, in each cell we assume the reaction takes place with probability $p_R = kn_An_B(n_B - 1)$, where n_α is the number of molecules of species α in a cell. The reactive dynamics in a cell is described by the Markov chain,[13]

$$P(\mathbf{n}, t + 1) = \sum_{\mathbf{n}'} W(\mathbf{n}|\mathbf{n}')P(\mathbf{n}', t) \tag{7}$$

where $\mathbf{n} = (n_A, n_B)$, $P(\mathbf{n}, t)$ is the probability that there are $\mathbf{n}$ particles in the cell at time t, and the transition matrix W is given by

$$\begin{aligned} W(\mathbf{n}|\mathbf{n}') = {} & kn'_An'_B(n'_B - 1)\delta_{n_A,n'_A-1}\delta_{n_B,n'_B+1} + \\ & (1 - kn'_An'_B(n'_B - 1))\delta_{n_A,n'_A}\delta_{n_B,n'_B} \end{aligned} \tag{8}$$

The (discrete time) rate of change of the mean density of species

α, $\bar{n}_\alpha(t) = \sum_{\mathbf{n}} n_\alpha P(\mathbf{n}, t)$, is

$$\bar{n}_\alpha(t+1) - \bar{n}_\alpha(t) = \sum_{\mathbf{n},\mathbf{n}'} n_\alpha (W(\mathbf{n}|\mathbf{n}') - \delta_{\mathbf{n},\mathbf{n}'}) P(\mathbf{n}, t) \quad (9)$$

We assume that the MPC nonreactive collisions are sufficiently effective to maintain a local equilibrium Poissonian distribution in the cells so that

$$P(\mathbf{n}, t) \approx P_l(n_A; \bar{n}_A(t)) P_l(n_B; \bar{n}_B(t)) \quad (10)$$

where the local Poisson distribution is $P_l(n; \bar{n}(t)) = e^{-\bar{n}(t)} \bar{n}(t)^n / n!$. If we insert the local Poissonian approximation for $P(\mathbf{n}, t)$ in the right-hand side of eq 9 for $\alpha = A$, we obtain the discrete-time mean-field rate law

$$\bar{n}_A(t+1) - \bar{n}_A(t) = -k \bar{n}_A(t) \bar{n}_B{}^2(t) \quad (11)$$

A similar equation can be derived for species B. Thus, the mass action rate law will describe the dynamics provided diffusion is sufficiently rapid compared to reaction so that a local Poissonian distribution of particles is maintained during the evolution of the reactive system. In this limit the discrete-time rate law will closely approximate the continuous-time mass action rate law.

After the reaction step, the particles free stream using the post-collision values of the velocities, taking into account the boundary conditions of the system. Once all the particles have been moved, the time advances one unit and the multiparticle collision and reaction steps are applied again. This mesoscopic dynamics conserves the total mass, momentum, and energy of the system.

3. Simulation of Chemical Fronts

In this section we show that the mesoscopic MPC model can be used simulate the dynamics of cubic autocatalytic fronts on macroscopic scales where comparisons with the predictions of reaction−diffusion equations can be made. Cubic autocatalytic fronts have been studied often in the context of a coupled pair of reaction−diffusion equations for the A and B species.[14−20] The particular focus of many of these studies was on the transverse front instability that occurs when the diffusion coefficient of the fuel is sufficiently larger than that of the autocatalyst: at a critical value of the diffusion coefficient ratio an instability will develop and the planar front will become nonplanar and exhibit complex dynamics.

Our investigations will be confined to a simpler case of a binary mixture undergoing the cubic autocatalytic reaction. For such a reacting mixture the relevant macroscopic field variables are the total mass density $\rho(\mathbf{r}, t) = \rho_A + \rho_B$, the local concentration $c(\mathbf{r}, t) = \rho_A/\rho$, the center of mass velocity $v(\mathbf{r}, t)$, and the energy density $e(\mathbf{r}, t)$. For the isothermal cubic autocatalytic reaction with no net fluid flow so that $v(\mathbf{r}, t) = 0$, and taking equal masses for the A and B species, the macroscopic equation for the number density of A is[21]

$$\frac{\partial}{\partial t} \bar{n}_A(\mathbf{r}, t) = -k \bar{n}_A \bar{n}_B{}^2 + D \nabla^2 \bar{n}_A \quad (12)$$

where D is the mutual diffusion coefficient. The equation for $\bar{n}_B(\mathbf{r}, t)$ is not independent and follows from number conservation, $\bar{n}_A + \bar{n}_B = \bar{n}_0$.

Front Profile. The simulations of the reaction front using the MPC model were carried out in a rectangular prism with length $l = 200$ along x, width $w = 200$ along y, and height $h = 5$ units along z. The system was open along its length x, periodic boundary conditions were imposed in the y-direction, and bounce-back reflection boundary conditions were imposed on the top and bottom of the prism along z. To initiate a chemical front, A particles were distributed uniformly in the right side of the prism, ($\bar{n}_A(x \geq 100) = 10$, $\bar{n}_B(x \geq 100) = 0$), while B particles were uniformly distributed in left side of the prism ($\bar{n}_A(x < 100) = 0$, $\bar{n}_B(x < 100) = 10$). The velocities were chosen from a Maxwell−Boltzmann distribution with reduced temperature $k_B T = \beta^{-1} = 1/3$.

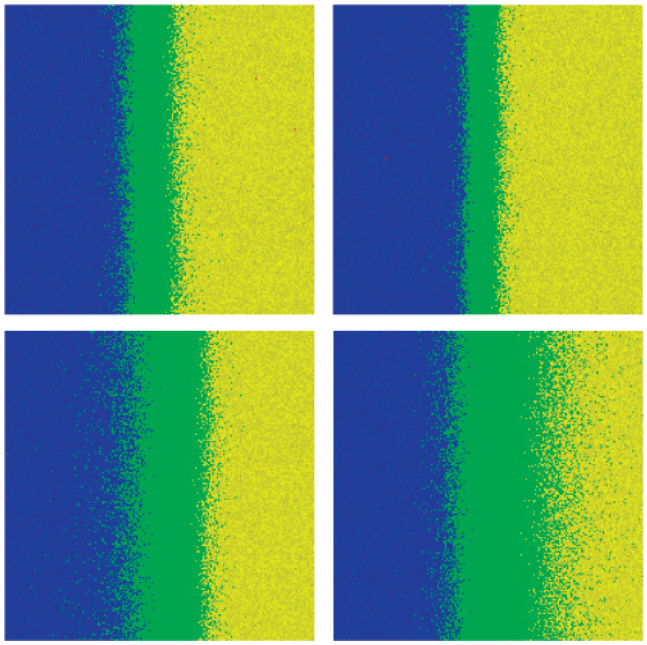

Figure 2. Concentration field at a given time instant for $k = 0.0005$ (top left panel) and $k = 0.001$ (top right panel). The system size is 200 × 200 × 5. Lower panels show the concentration field for $k = 0.0005$ and $\gamma_A = 0.25$, $\gamma_B = 1$ (left), and $k = 0.0005$, $\gamma_A = 1$, $\gamma_B = 0.25$ (right). The structure of the reaction zone can be seen in these figures.

Starting from this initial condition, a reaction front will develop as the autocatalyst B consumes the fuel A in the reaction. The front will move with velocity c, and it is convenient to study the front dynamics in a frame moving with velocity c. Propagating fronts are depicted in Figure 2, which shows the concentration field at a given time instant. The upper two panels plot the front for two values of the reaction rate constant k and $\gamma_A = \gamma_B = 1$. We see that for $k = 0.0005$ the front profile is much thicker than that for $k = 0.001$. This dependence is in accord with predictions based on a reaction−diffusion description of the front as can be seen from the analysis given below.

The structure of these planar fronts can be investigated quantitatively by studying the front dynamics in a frame moving with the front velocity, $\xi = x - ct$ and averaging the concentration profile over the width (along y) of the front, $\bar{n}_A(\xi) = \int dy\, n_A(\xi, y)$. Figure 3 plots $\bar{n}_A(\xi)$ for the two values of k used in Figure 2. From this figure we see that a well-defined propagating reaction front is obtained and the width of the front decreases as the reaction rate increases relative to the diffusion rate.

The front shape and velocity can be determined from the reaction−diffusion equation. For a planar front propagating along the x-direction, in a frame moving with the front velocity,

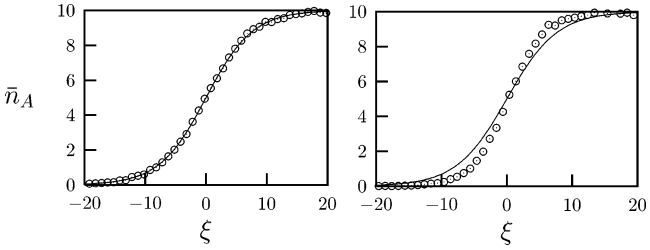

Figure 3. Plot of the front profile $\bar{n}_A(\xi)$ versus ξ for different values of k: left panel, $k = 0.0005$; right panel, $k = 0.001$. The system size is $200 \times 200 \times 5$. The continuous line represents the theoretical value obtained from eq 14.

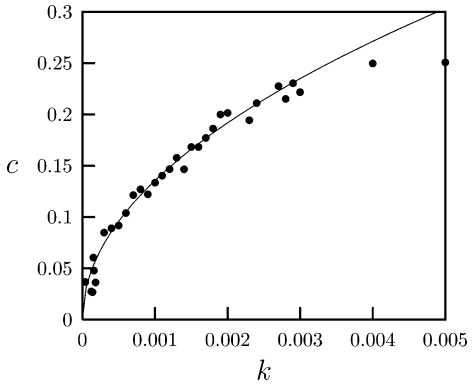

Figure 4. (filled circles) Front velocity c as a function of k. (solid line) Front velocity from eq 14.

the reaction−diffusion eq 12 is

$$D\frac{d^2}{d\xi^2}\bar{n}_A(\xi) + c\frac{d}{d\xi}\bar{n}_A(\xi) - k\bar{n}_A(\xi)(\bar{n}_0 - \bar{n}_A(\xi))^2 = 0 \qquad (13)$$

The front profile can be found analytically from the solution of this equation and is given by[20]

$$\bar{n}_A(\xi) = \bar{n}_0(1 + e^{-c\xi/D})^{-1} \qquad (14)$$

where the front speed is $c = (Dk\bar{n}_0^2/2)^{1/2}$. The profile for species B can be found from the conservation condition $\bar{n}_A + \bar{n}_B = \bar{n}_0$. Figure 3 compares this analytical prediction with the simulation results of the MPC reaction−diffusion dynamics. For $\gamma_A = \gamma_B = 1$ the mutual diffusion coefficient D is given by eq 5. There is good agreement between the simulation and analytical values for small k where the conditions for the validity of the mean field approximation are satisfied. For larger k values, such as $k = 0.001$ in the right panel of the figure we see that there are deviations from the mean field result. For this value of k, the reaction is fast and there is a breakdown of the local Poissonian equilibrium and a reaction−diffusion description is not applicable. A similar breakdown is observed for very small k, for example for $k = 0.0002$, due to the fact that very few reactive events occur in the reaction zone of the front and fluctuations are important.

The front velocity was determined from the simulation data as a function of k. In Figure 4 we plot the front velocity c versus k and compare the simulation results with the prediction $c = (Dk\bar{n}_0^2/2)^{1/2}$. The front velocity agrees with the simulation results for $k \leq 0.003$, although the front profile deviates slightly from the predicted value for somewhat smaller values of k ($k \leq 0.001$).

More microscopic aspects of the front structure and dynamics that are captured by the MPC model are illustrated in the lower two panels of Figure 2. These figures plot snapshots of the front for $k = 0.0005$, the same value of k as in the top left panel of the figure, but for two different pairs of γ_α values, ($\gamma_A = 0.25$, $\gamma_B = 1.0$) and ($\gamma_A = 1.0$, $\gamma_B = 0.25$). Comparison of the lower panels of the figures, and also with the upper left panel, shows that the structures of the interfacial zones are different. In the MPC dynamics employed here, the diffusion of the species depends on their density and γ_α. Since the density of the species changes significantly in the interfacial zone, it is likely that a concentration-dependent mutual diffusion coefficient is required to describe this structure.

4. Conclusion

The generalizations of the multiparticle collision model described here, and its extensions, allow one to study a variety of phenomena at the mesoscopic level. In particular, the ability to simulate the dynamics of multicomponent systems, whose diffusion coefficients can be different, means that diffusion-driven instabilities, such as the transverse cubic autocatalytic front instability considered in this paper, can be investigated. Since the mesoscopic MPC model preserves the basic conservation laws in the system, to study such instabilities requires the presence of a third solvent species so that there are two independent diffusion coefficients in the system. The method could also be used to study reactive and nonreactive binary fluid *flows*, which also show interesting instabilities where fluctuations play a role near the onset of instabilities.

The cubic autocatalytic reaction is simply one example of a much broader class of reaction−diffusion systems that can be studied using reactive versions of the mesoscopic multiparticle collision dynamics. In particular, more general reaction−diffusion dynamics in specific geometries relevant for the materials science and biological applications may be carried out. The presence of flows can also be treated easily in this context.

While we have focused primarily on parameter domains where mean field approximations are largely applicable, one of the most interesting applications of the methodology introduced in this paper is to systems on mesoscales where particle numbers are small so that fluctuations play a crucial role in the dynamics and system geometry is important.

Acknowledgment. This work was supported in part by a grant from the Natural Sciences and Engineering Research Council of Canada (R.K.) and by the grant C-1279-0402-B from Consejo de Desarrollo Cientfico Humanstico y Tecnolgico of Universidad de Los Andes (K.T.).

References and Notes

(1) Nicolis, G.; Prigogine, I. *Self-Organization in Non-Equilibrium Systems*; Wiley: New York, 1977.
(2) Malevanets, A.; Kapral, R. *Europhys. Lett.* **1998**, *44*(5), 552.
(3) Malevanets, A.; Kapral, R. *J. Chem. Phys.* **1999**, *110*, 8605.
(4) Malevanets, A.; Kapral, R. *J. Chem. Phys.* **2000**, *112*, 7260.
(5) Malevanets, A.; Kapral, R. *Lect. Notes Phys.* **2004**, *640*, 113.
(6) Ihle, T.; Kroll, D. M. *Phys. Rev. E* **2001**, *63*, 020201. Lamura, A.; Gompper, G.; Ihle, T.; Kroll, D. M. *Europhys. Lett.* **2001**, *56*, 768. Lamura, A.; Gompper, G.; Ihle, T.; Kroll, D. M. *Europhys. Lett.* **2001**, *56*, 319.
(7) Hashimoto, Y.; Chen, Y.; Ohashi, H. *Comput. Phys. Comm.* **2000**, *129*, 56. Inoue, Y.; Chen, Y.; Ohashi, H. *Colloids Surf. A* **2002**, *201*, 297. Sakai, T.; Chen, Y.; Ohashi, H. *Phys. Rev. E* **2002**, *65*, 031503.
(8) Malevanets, A.; Yeomans, J. M. *Europhys. Lett.* **2000**, *52*, 231.
(9) Lee, S. H.; Kapral, R. *J. Chem. Phys.* **2004**, *121*, 11163.
(10) Tucci, K.; Kapral, R. *J. Chem. Phys.* **2004**, *120*, 8262.
(11) Malevanets, A.; Yeomans, J. M. *Comput. Phys. Commun.* **2000**, *129*, 282.
(12) Gardiner, C. W. *Handbok of Stochastic Processes*; Springer-Verlag: New York, 1985.
(13) Kapral, R. In *Stochastic Dynamics*; Shimansky-Geier, L., Pöschel, T., Eds.; Springer: Berlin, 1997; p 294.
(14) Horváth, D.; Showalter, K. *J. Chem. Phys.* **1995**, *102*, 2471.

(15) Billingham, J.; Needham, D. J. *Philos. Trans. R. Soc., Ser. A* **1991**, *334*, 1.
(16) Scott, S. K.; Showalter, K. *J. Phys. Chem.* **1992**, *96*, 8702.
(17) Horváth, D.; Petrov, V.; Scott, S. K.; Showalter, K. *J. Chem. Phys.* **1993**, *98*, 6332.
(18) Zhang, Z.; Falle, S. A. E. G. *Proc. R. Soc., Ser. A* **1994**, *446*, 1.
(19) Milton, R. A.; Scott, S. K. *J. Chem. Phys.* **1995** *102*, 5271.
(20) Malevanets, A.; Careta, A.; Kapral, R. *Phys. Rev. E* **1995**, *52*, 4724.
(21) de Groot, S. R.; Mazur, P. *Nonequilibrium Thermodynamcis*; North-Holland: Amsterdam, 1962.